The Spin-2 AKLT State on the Square Lattice is Universal for Measurement-based Quantum Computation*

Tzu-Chieh Wei[1] and Robert Raussendorf[2]

1 **C. N. Yang Institute for Theoretical Physics and Department of Physics and Astronomy**
State University of New York at Stony Brook, Stony Brook, NY 11794-3840, USA
tzu-chieh.wei@stonybrook.edu

2 **Department of Physics and Astronomy, University of British Columbia**
Vancouver, British Columbia, V6T 1Z1, Canada
rrausen@phas.ubc.ca

Abstract

One-way quantum computation was first invented using the cluster state. Since then graph states, the generalization of the cluster state, were investigated and understood when they would enable such a measurement-based approach for quantum computation. Are there any other family of states, i.e., states with different entanglement structures, that can also serve as the universal resource for quantum computation? Recent study shows that the Affleck-Kennedy-Lieb-Tasaki (AKLT) states also provide a useful source. Here, we show that the spin-2 state on the square lattice is a universal resource for measurement-based quantum computation. We employ a POVM on all sites that convert the local 5-level system to 2-level, and the post-POVM state is a graph state, whose graph is in general non-planar. We then follow with another round of measurement to recover the planarity of the graphs by thinning. The resultant typical graphs are shown to reside in the supercritical phase of percolation via Monte Carlo simulations and the associated graph states are universal, implying the AKLT state is also universal.

1998 ACM Subject Classification F.1.1 Models of Computation

Keywords and phrases Measurement-based quantum computation, AKLT state, graph state, percolation

Digital Object Identifier 10.4230/LIPIcs.TQC.2015.48

1 Introduction and motivation

Universal quantum computation can be achieved by using local measurements on certain entangled states, such as the cluster state. This measurement-based model of quantum computation (MBQC) [13, 1, 14] provides equivalent power of computation as the standard circuit model. However, not all entangled states can provide the capability for driving a universal quantum computation. A complete classification of entanglement that enables MBQC remains a challenging open question. The quest for more universal resource states will advance our knowledge towards the essential type of entanglement. The family of cluster states or more generally graph states contains abundance supply of resource states. These

* This work was partially supported by NSF, NSERC, Cifar and PIMS.

10th Conference on the Theory of Quantum Computation, Communication and Cryptography (TQC 2015).
Editors: Salman Beigi and Robert König; pp. 48–63

Leibniz International Proceedings in Informatics
Schloss Dagstuhl – Leibniz-Zentrum für Informatik, Dagstuhl Publishing, Germany

states, however, cannot be unique ground states of two-body interacting Hamiltonians [12]. Beyond this family of states, only a handful of other entangled states are known to be universal [6, 3, 2, 10].

Here, we demonstrate that the spin-2 Affleck-Kennedy-Lieb-Tasaki (AKLT) state on the square lattice is a universal resource for measurement-based quantum computation (MBQC). This question has been open since the universality of the spin-3/2 AKLT state on the honeycomb lattice was established [16, 11]. AKLT states can be defined on any graph and are unique ground states of two-body interacting Hamiltonians with suitable boundary conditions. But the quantum computational universality in this family is less explored than the family of cluster or graph states. Together with the results here, the emerging picture from a series of study on the quantum computational universality in the AKLT valence-bond family is as follows [16, 11, 17, 15, 18]. AKLT states involving spin-2 and other lower spin entities are universal if they reside on a frustration-free lattice with any combination of spin-2, spin-3/2, spin-1 and spin-1/2 (consistent with the lattice). Additionally, a frustrated lattice can always be decorated (by adding additional spins) such that the resultant AKLT state is universal.

2 Overall strategy

Our goal is to show that any quantum computation that is efficiently implemented in the circuit model can also be implemented efficiently by a sequence of adaptive local measurements on a spin-2 AKLT state. In other words, we want to show that the spin-2 AKLT state is a universal resource for MBQC.

The overall strategy for demonstrating this is: (1) we need to find a POVM that converts a 5-level state to a 2-level state; (2) we show that the post-POVM state is a graph state; (3) if this graph state has a planar graph then we check whether the graph is percolated; if the graph is non-planar, we need to restore planarity by apply futher active local measurement.

However, it is not guaranteed that the POVM will convert the AKLT state a qubit graph state. Fortunately, the POVM we found in Eq. (1) below allows us to do this. The graphs associated with the post-POVM states are generally not planar and we indeed need to apply some procedure to restore planarity at the cost of measuring and disentangling more qubits. In order to show that the typical graphs are percolated, we need to sample from the exact distribution. For this we manage to prove an exact weight formula for any given POVM outcome, and this allows us to perform Monte Carlo simulations. The most pronounced difference between the spin-3/2 and spin-2 probability weights is that for spin 3/2 all possible combinations of POVM outcomes do indeed occur with non-zero probability (except when the lattice is not bi-colorable) whereas, for the spin-2 case, certain combinations of POVM outcomes do not occur, i.e., have probability zero.

Why our work is interesting? We investigate how particular condensed-matter spin systems (the AKLT family) can be exploited for quantum computation. The framework is the so-called measurement-based quantum computation, one of several experimentally pursued approaches for realizing a quantum computer, which uses entanglement as a resource. Proving a general state can be useful in measurement-based quantum computation remains a theoretical challenge. Our present manuscript represents a significant advancement since our paper in 2011 [16], and together with our other recent works, gives a comprehensive understanding of why some generic states in the so-called AKLT family are useful. AKLT states are important from many perspectives: strong evidence for Haldane's conjecture, precursor of

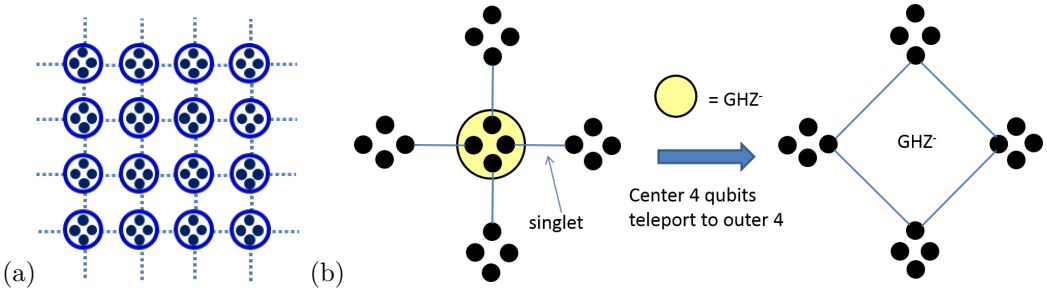

Figure 1 (a) AKLT state. Spin singlets $|\phi\rangle_e = (|01\rangle - |10\rangle)/\sqrt{2}$ of two virtual spins 1/2 are located on the edges of the square lattice. A projection at each lattice site onto the symmetric subspace of four virtual spins creates the AKLT state. (b) Teleportation. A perspective of the action of the POVM K_α in Eq. (1).

the so-called matrix product states and tensor product states (which have been developed to useful numerical tools), examples of symmetry-protected topological ordered states, and with our contribution, quantum computation, etc. We believe our paper is of interest to researchers in various fields, including condensed-matter physics, quantum information and computation, AMO physics (as possible implementation and indeed a proof-of-principle demonstration on 1D AKLT quantum computation was done with entangled photons [8]), statistical mechanics (given some of the techniques we used), and mathematics (such as random graph and probability theory).

3 Reduction from AKLT states to graph states

Let us define the AKLT state on the square lattice. It is useful to view the spin-2 particle on each site is consisting of four virtual qubits. Each virtual qubit forms a singlet state, $|\phi\rangle_e = (|01\rangle - |10\rangle)/\sqrt{2}$, with its corresponding virtual qubit on the neighboring site, with the singlets indicated by the dotted edges; see Fig. 1a. In order to convert the local 5-level system to 2-level, we shall use a POVM measurement below in Sec. 3.1. We shall see that regardless of the POVM outcome, the post-measurement state is a graph state, with its graph being modified from the original square lattice, more or less, randomly. However, the graph is not planar. But it is easier to understand such graphs as resulting from a two-step process: (1) a planar random graph from the square lattice is formed (which we prove in Sec. 3.2); then (2) certain Pauli measurements (due to some of the POVM elements) are then done to change the graph further (which we illustrate in Sec. 3.3).

3.1 Reduction from spin-2 entities to qubits: the generalized measurement

The POVM we shall employ consists of three rank-two elements and three additional rank-one elements [18]:

$$F_\alpha = \sqrt{\frac{2}{3}}\,(|S_\alpha{=}2\rangle\langle S_\alpha{=}2| + |S_\alpha{=}{-}2\rangle\langle S_\alpha{=}{-}2|), \quad K_\alpha = \sqrt{\frac{1}{3}}\,|\phi_\alpha^-\rangle\langle\phi_\alpha^-|, \tag{1}$$

where $\alpha = x, y, z$ and $|\phi_\alpha^\pm\rangle \equiv (|S_\alpha{=}2\rangle \pm |S_\alpha{=}{-}2\rangle)/\sqrt{2}$. The F's are straightforward generalization from the spin-3/2 case [16], but they do not give rise to the completeness relation, which is required for conservation of probabilities. By adding K's, it can be verified that the completeness relation is satisfied: $\sum_\alpha F_\alpha^\dagger F_\alpha + \sum_\alpha K_\alpha^\dagger K_\alpha = I$.

Expressed in terms of the four virtual qubits representing a spin-2 particle, the above operators in the POVM are

$$F_x = \sqrt{\tfrac{2}{3}}(|+^{\otimes 4}\rangle\langle +^{\otimes 4}| + |-^{\otimes 4}\rangle\langle -^{\otimes 4}|), \qquad K_x = \sqrt{\frac{1}{3}}|\mathrm{GHZ}_{\mathrm{x}}^-\rangle\langle \mathrm{GHZ}_{\mathrm{x}}^-|, \tag{2a}$$

$$F_y = \sqrt{\tfrac{2}{3}}(|i^{\otimes 4}\rangle\langle i^{\otimes 4}| + |(-i)^{\otimes 4}\rangle\langle (-i)^{\otimes 4}|), \qquad K_y = \sqrt{\frac{1}{3}}|\mathrm{GHZ}_{\mathrm{y}}^-\rangle\langle \mathrm{GHZ}_{\mathrm{y}}^-|, \tag{2b}$$

$$F_z = \sqrt{\tfrac{2}{3}}(|0^{\otimes 4}\rangle\langle 0^{\otimes 4}| + |1^{\otimes 4}\rangle\langle 1^{\otimes 4}|), \qquad K_z = \sqrt{\frac{1}{3}}|\mathrm{GHZ}_{\mathrm{z}}^-\rangle\langle \mathrm{GHZ}_{\mathrm{z}}^-|, \tag{2c}$$

where $|\psi^{\otimes 4}\rangle$ is a short-hand notation for $|\psi,\psi,\psi,\psi\rangle$, equivalent to an eigenstate $|S_\alpha\rangle$ of the spin-2 operator in either $\alpha = \mathrm{x}$, y, or z direction. The first three elements are similar to those in spin-3/2 sites, except the number of virtual qubits being four, and correspond to good outcomes of type x, y and z, respectively. Associated with the last three elements, $|\mathrm{GHZ}_{\mathrm{z}}^-\rangle \equiv (|0000\rangle - |1111\rangle)/\sqrt{2}$, $|\mathrm{GHZ}_{\mathrm{x}}^-\rangle \equiv (|++++\rangle - |----\rangle)/\sqrt{2}$, and $|\mathrm{GHZ}_{\mathrm{y}}^-\rangle \equiv (|\mathrm{i},\mathrm{i},\mathrm{i},\mathrm{i}\rangle - |-\mathrm{i},-\mathrm{i},-\mathrm{i},-\mathrm{i}\rangle)/\sqrt{2}$ are the corresponding states and they will be regarded as unwanted outcomes of type x, y, and z, respectively. The effect of these GHZ outcomes is that the neighboring four virtual qubits connected to the center site becomes GHZ entangled, as illustrated in Fig. 1b. It is these GHZ entanglement in the virtual qubits that complicates the measurement-based quantum computation. The reduced density matrix for a single site of the AKLT state is a completely mixed state, and therefore, each unwanted type occurs on average with a probability 1/15. An unwanted outcome associated with K thus occurs with probability $p_{\mathrm{err}} = 3 \times 1/15 = 1/5$. However, as we shall see below in Sec. 5 that not all POVM outcomes associated with sets of $\{F_{\alpha(v)}, K_{\beta(w)}\}$ occur with non-zero probability, due to the correlation present in the AKLT state.

We note that K_α can be rewritten as follows,

$$K_\alpha = \sqrt{1/2}|\phi_\alpha^-\rangle\langle\phi_\alpha^-|F_\alpha = \sqrt{2/3}\, K_\alpha F_\alpha. \tag{3}$$

We can thus think of the POVM Eq. (1) as a two-stage process: (i) first the outcomes on all sites are F's, and (ii) then a number of sites are flipped to K or equivalently a projective measurement is done in the basis $|\phi_\alpha^\pm\rangle$ and the result $|\phi_\alpha^-\rangle$ is post-selected.

Corresponding to step (i), we show in the next section that the post-measurement state

$$\overline{|G_0(\{F\})\rangle} \sim \bigotimes_{v\in\mathcal{L}} F_{\alpha(v)}|\psi_{\mathrm{AKLT}}\rangle \tag{4}$$

is an encoded graph state [16, 17]. The 'bar' is used to indicate that the graph state is 'encoded', i.e., one logical qubit is formed by a few physical spins which we also can a *domain*. We shall omit the bar and write the state as $|G_0\rangle$ instead. In the section after that, we discuss the effect of K's, which is either simply shrinking the size of a domain or inducing a Pauli measurement.

3.2 The exact form of stabilizer generators

In this section we prove that $|G_0\rangle$ is a graph state by deriving the form of the stabilizer operators $\mathcal{K}_c$ for the domain labeled by $\mathcal{C}_c$. It includes all subtle plus and minus signs. The result is general for all states $|G_0\rangle \sim \bigotimes_{v\in\Omega} F_{\alpha_v,v}|\psi_{\mathrm{AKLT}}\rangle$, where F's can be of arbitrary spins. This was already considered in the case of the spin-3/2 AKLT state [16], but the argument used there applies more generally.

Let us first explain the notation. Consider a central vertex $\mathcal{C}_c \in V(G_0(\{F\}))$ and all its neighboring vertices $\mathcal{C}_\mu \in V(G_0)$; see e.g. Fig. 2 for illustration. Each vertex may contain

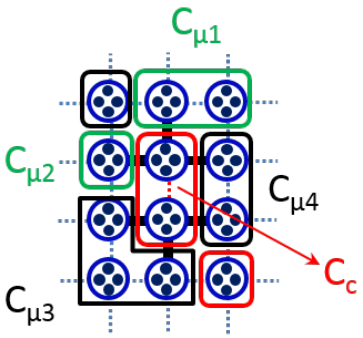

Figure 2 POVM outcomes. The center domain $\mathcal{C}_c$ has $a_c = x$ (red), and its neighboring domains: $\mathcal{C}_{\mu 1}$ and $\mathcal{C}_{\mu 2}$ have $a_{\mu 1} = a_{\mu 2} = y$ (green); $\mathcal{C}_{\mu 3}$ and $\mathcal{C}_{\mu 4}$ have $a_{\mu 3} = a_{\mu 4} = z$ (black).

multiple sites that are connected and are of the same POVM outcome F_α. We shall refer to these sites collectively as a *domain*. Namely, each vertex in graph G_0 is physically a domain. Denote the POVM outcome for all $\mathcal{L}$-sites $v \in \mathcal{C}_c, \mathcal{C}_\mu$ by a_c and a_μ, respectively. Denote by E_μ the set of $\mathcal{L}$-edges that run between $\mathcal{C}_c$ and $\mathcal{C}_\mu$. Denote by E_c the set of $\mathcal{L}$-edges internal to $\mathcal{C}_c$. Denote by C_c the set of all qubits in $\mathcal{C}_c$, and by C_μ the set of all qubits in $\mathcal{C}_\mu$. (Recall that there are 4 qubit locations per $\mathcal{L}$-vertex $v \in \mathcal{C}_c, \mathcal{C}_\mu$.) For any μ and any edge $e \in E_\mu$, let $u(e)$ $[v(e)]$ be the endpoint of e in C_μ $[C_c]$. Then, for all μ and all $e \in E_\mu$ the Pauli operators $-\sigma_{a_\mu}^{(u(e))}\sigma_{a_\mu}^{(v(e))}$ are in the stabilizer of the singlet $\bigotimes_{e\in E(\mathcal{L})} |\phi\rangle_e$.

Choose $b \in \{x, y, z\}$ such that $b \neq a_c$, and let, for any edge $e' \in E_c$, $v_1(e'), v_2(e') \in C_c$ be qubit locations such that $e' = (v_1(e'), v_2(e'))$. Then, for all $e' \in E_c$, $-\sigma_b^{(v_1(e'))}\sigma_b^{(v_2(e'))}$ is in the stabilizer of $\bigotimes_{e\in E(\mathcal{L})} |\phi\rangle_e$.

Thus we have the following operator as the stabilizer for $\bigotimes_{e\in E(\mathcal{L})} |\phi\rangle_e$,

$$\begin{aligned}\mathcal{K}_c &= \bigotimes_\mu \bigotimes_{e\in E_\mu} (-1)\sigma_{a_\mu}^{(u(e))}\sigma_{a_\mu}^{(v(e))} \bigotimes_{e'\in E_c} (-1)\sigma_b^{(v_1(e'))}\sigma_b^{(v_2(e'))} \\ &= (-1)^{|E_c|+\sum_\mu |E_\mu|} \bigotimes_\mu \bigotimes_{e\in E_\mu} \sigma_{a_\mu}^{(u(e))}\sigma_{a_\mu}^{(v(e))} \bigotimes_{e'\in E_c} \sigma_b^{(v_1(e'))}\sigma_b^{(v_2(e'))}.\end{aligned}$$

We now show that $O_{\mathcal{C}_c}$ commutes with the local POVMs and is therefore also in the stabilizer of $|\Psi(\mathcal{A})\rangle$. First, consider the central domain $\mathcal{C}_c$. The operator $O_{\mathcal{C}_c}$ acts non-trivially on every qubit in C_c, $O_{\mathcal{C}_c}|_l \neq I_l$ for all qubits $l \in C_c$. Furthermore, for all qubits $l \in C_c$, $O_{\mathcal{C}_c}|_l \neq \sigma_{a_c}^{(l)}$. Namely, if $l \in C_c$ is connected by an edge $e \in E_\mu$ to $\mathcal{C}_\mu$, for some μ, then $O_{\mathcal{C}_c}|_l = \sigma_{a_\mu}^{(l)} \neq \sigma_{a_c}^{(l)}$ (for all μ, $a_\mu \neq a_c$ by construction of $G(\mathcal{A})$). Or, if $l \in C_c$ is the endpoint of an internal edge $e' \in E_c$ then $O_{\mathcal{C}_c}|_l = \sigma_b^{(l)} \neq \sigma_{a_c}^{(l)}$ ($a_c \neq b$ by above choice). Therefore, for any $i, j \in C_c$, $O_{\mathcal{C}_c}$ anticommutes with $\sigma_{a_c}^{(i)}$ and $\sigma_{a_c}^{(j)}$, and thus commutes with all $\sigma_{a_c}^{(i)}\sigma_{a_c}^{(j)}$. Thus, $O_{\mathcal{C}_c}$ commutes with the local POVMs F_{a_c} in Eq. (2) on all $v \in \mathcal{C}_c$.

Second, consider the neighboring domains $\mathcal{C}_\mu$. $O_{\mathcal{C}_c}|_{\mathcal{C}_\mu} = \bigotimes_j \sigma_{a_\mu}^{(j)}$ by construction. $O_{\mathcal{C}_0}$ thus commutes with the local POVMs F_{v,a_μ} for all $v \in \mathcal{C}_\mu$ and for all μ.

To give explicit form of the stabilizer operators, we shall take the following convention for b as shown in Table 1. For POVM outcome $a_c = z$, we take $b = x$; for $a_c = x$, we take $b = z$; for $a_c = y$, we take $b = z$. With this choice we have

$$\mathcal{K}_c = (-1)^{|E_c|+\sum_\mu |E_\mu|} \bigotimes_\mu (\otimes_{e\in E_\mu} \lambda_{u(e)}) Z_\mu^{|E_\mu|} \bigotimes_{e\in E_\mu} \sigma_{a_\mu}^{v(e)}\sigma_b^{v(e)} X_c.$$

Table 1 The choice of b and $a_{\mu\neq b}$.

a_c	z	x	y
b	x	z	z
$a_{\mu\neq b}$	y	y	x

Table 2 The dependence of stabilizers and encodings on the local POVM outcome. $|\mathcal{C}|$ denotes the total number of sites contained in a domain $\mathcal{C}$ and $i,j = 1\,..\,4|\mathcal{C}|$ (as there are four vitural qubits in a site). The square lattice $\mathcal{L}$ is bi-partite and all sites can be divided into either A or B sublattice, $V(\mathcal{L}) = A \cup B$, and $\lambda_i = 1$ if the virtual qubit $i \in v \in A$ and $\lambda_i = -1$ if $i \in v' \in B$. This is due to the negative sign in the stabilizer generator for a singlet $|\phi\rangle_{ij}$, $(-\sigma_\mu^{[i]}\sigma_\mu^{[j]})|\phi\rangle_{ij} = |\phi\rangle_{ij}$ for an edge (i,j).

POVM outcome	z	x	y
stabilizer generator	$\lambda_i\lambda_j\sigma_z^{[i]}\sigma_z^{[j]}$,	$\lambda_i\lambda_j\sigma_x^{[i]}\sigma_x^{[j]}$	$\lambda_i\lambda_j\sigma_y^{[i]}\sigma_y^{[j]}$
$\overline{X}$	$\bigotimes_{j=1}^{4\|\mathcal{C}\|}\sigma_x^{[j]}$	$\bigotimes_{j=1}^{4\|\mathcal{C}\|}\sigma_z^{[j]}$	$\bigotimes_{j=1}^{4\|\mathcal{C}\|}\sigma_z^{[j]}$
$\overline{Z}$	$\lambda_i\sigma_z^{[i]}$	$\lambda_i\sigma_x^{[i]}$	$\lambda_i\sigma_y^{[i]}$

It is convenient to define $n_{\neq b} \equiv \sum_{\mu, a_\mu\neq b}|E_\mu|$. Then

$$\mathcal{K}_c \quad = \quad (-1)^{|E_c|+\sum_\mu |E_\mu|}\bigotimes_\mu(\otimes_{e\in E_\mu}\lambda_{u(e)})Z_\mu^{|E_\mu|}(\bigotimes_{a_\mu\neq b}\otimes_{e\in E_\mu}\lambda_{v(e)})Q_c, \tag{5}$$

where $Q_c = i^{n_{\neq b}}X_c$ if $n_{\neq b}$ is even and $Q_c = -i^{1+n_{\neq b}}(-1)^{\delta_{a_c,x}}Y_c$ if $n_{\neq b}$ is odd. This gives complete characterization of stabilizer generators, i.e., $Q_c = \pm X_c$ or $Q_c = \pm Y_c$ and the exact sign can be determined. This is essential in checking the incompatibility condition.

Note that the stabilizer operators are not always in the canonical form in which $\mathcal{K}_c|_c = X_c$, i.e., they can be $\pm X_c$ or $\pm Y_c$, but those non-central operators are always Z. But it is easy to find rotations (around logical z-axis) to make them canonical. We shall the basis after such rotations are made the canonical graph-state basis (CGSB).

A few remarks are in order.

1. Each domain on $\mathcal{L}$ supports a single encoded qubit, i.e., the domains $D \subset \mathcal{L}$ are the sites or vertices of the graph G_0, with the encoding as described in Table 2. The encoded qubits form a graph state $\overline{|G_0\rangle}$. When there is no confusion, we shall not distinguish between the graph state $|G_0\rangle$ and its encoded version $\overline{|G_0\rangle}$ and omit the labeling $\{F\}$.
2. The graph G_0 has an edge between the vertices $v(D)$ and $v(D')$, if the domains D and D' are connected by an odd number of edges in $\mathcal{L}$.
3. Be D a domain of type $T \in \{x,y,z\}$ with n_α neighbouring domains of type α. The stabilizer operators for such a graph state are shown in Eq. (5) in terms of encoded logical operators. They are characterized by the so-called stabilizer matrix, and in the case of graph state, is given via the adjacency matrix A_{G_0} of the graph G_0. It is seen that when

$$\begin{aligned} n_y \mod 2 &= 1, \quad \text{for } T = x, \\ n_x \mod 2 &= 1, \quad \text{for } T = y, \\ n_y \mod 2 &= 1, \quad \text{for } T = z, \end{aligned}$$

the stabilizer operator $\mathcal{K}_D$ has a logical Y operator at the support of D. This means that the graph G_0 has a self-loop attached to the domain D, i.e., $(A_{G_0})_{D,D} = 1$.

We recall the definition of a "domain". A domain is a maximal set of neighbouring sites in the lattice $\mathcal{L}$ for which the outcome of the POVM Eq. (1) is F_α or K_α [see Eq. (3)] with

the same α. That is, there are domains of x, y and z-type, and neighbouring domains must be of different type. The self-loop is a convenient picture to visualize the graph. But we can perform local logical rotation to transform Y to X so as to remove the self-loop, then the resulting stabilizer operators will be in the canonical form. (Such rotation will also change the basis of logical measurement.) Moreover, we shall often not distinguish between an encoded $\overline{X}$ or $\overline{Y}$ operator from the corresponding X or Y operator, unless necessary.

3.3 POVM outcomes K_α: domain shrinking and logical Pauli measurements

We shall denote by $\{F, K\}$ the POVM outcomes on all sites, by $J_F \subset \mathcal{L}$ the set of sites where the POVM outcome is of F-type, and by $J_K = \mathcal{L}\backslash J_F$ the set of sites where POVM outcome is of K-type. Upon obtaining $\{F, K\}$ we can deduce the state $|G\rangle$ that the original AKLT state is transformed to,

$$|G(\{F,K\})\rangle = \left(\sqrt{\frac{1}{2}}\right)^{|J_K|} \bigotimes_{u\in J_K} |\phi^-_{\alpha(u)}\rangle\langle\phi^-_{\alpha(u)}| \bigotimes_{v\in\mathcal{L}} F_{\alpha(v)}|\psi_{\rm AKLT}\rangle, \tag{6}$$

where the state is not normalized and the probability of the set of POVM outcomes $\{F, K\}$ occurs is

$$p(\{F,K\}) = \langle G(\{F,K\})|G(\{F,K\})\rangle. \tag{7}$$

We have shown that $|G_0\rangle$ is a graph state, and one can further show the normalization due to F's acting on the AKLT state [16],

$$\bigotimes_{u\in\mathcal{L}} F_{\alpha(u)}|\psi_{\rm AKLT}\rangle = c_0 \left(\frac{1}{\sqrt{2}}\right)^{|\mathcal{E}|-|V|} |G_0\rangle, \tag{8}$$

where c_0 is an outcome-independent overall normalization, V is the set of domains, $\mathcal{E}$ is the set of inter-domain edges (before the modulo-2 operation) and $|G_0\rangle$ is properly normalized to have unit norm [16]. For the encoding using virtual-qubit picture, see Table 2.

Summarizing the above discussion, we have

$$|G(\{F,K\})\rangle = c_0 \left(\sqrt{\frac{1}{2}}\right)^{|\mathcal{E}|-|V|+|J_K|} \left(\bigotimes_{u\in J_K} |\phi^-_{\alpha(u)}\rangle\langle\phi^-_{\alpha(u)}|\right) |G_0(\{F\})\rangle, \tag{9}$$

where $|G_0(\{F\})\rangle$ is assumed to be properly normalized. Without the additional operators $\bigotimes_{u\in J_K} |\phi^-_{\alpha(u)}\rangle\langle\phi^-_{\alpha(u)}|$ the analysis of the computational universality would be the same as in the spin-3/2 case. It is these operators that complicate the situtation. However, as we shall see below their effect is not serious.

Then the effect of measuring in the basis $|\phi^\pm_\alpha\rangle$ corresponds to shrinking or thinning the domain, without affecting the entanglement of the domain with others. This can be understood from the following example. Suppose a two-site domain with $\alpha = x$: the basis states are $|S_x = +2\rangle_1|S_x = -2\rangle_2$ and $|S_x = -2\rangle_1|S_x = +2\rangle_2$, due to the POVM. Let us denote the whole wavefunction of the system as $|\Psi\rangle = a\,|+2\rangle_1|-2\rangle_2 \otimes |\psi_0\rangle_R + b\,|-2\rangle_1|+2\rangle_2 \otimes |\psi_1\rangle_R$, where $|\psi_i\rangle_R$'s denote the corresponding state of other spins. We can rewrite the first spin in $|\phi^\pm_x\rangle$ basis: $|\Psi\rangle = |\phi^+_x\rangle\big(a\,|-2\rangle_2 \otimes |\psi_0\rangle_R + b\,|+2\rangle_2 \otimes |\psi_1\rangle_R\big)/\sqrt{2} + |\phi^-_x\rangle\big(a\,|-2\rangle_2 \otimes |\psi_0\rangle_R - b\,|+2\rangle_2 \otimes |\psi_1\rangle_R\big)/\sqrt{2}\big)$. The measurement outcome $\pm$ gives rise the reduced state being $a\,|-2\rangle_2 \otimes |\psi_0\rangle_R \pm b\,|+2\rangle_2 \otimes |\psi_1\rangle_R$. The only difference is that the domain is reduced to a

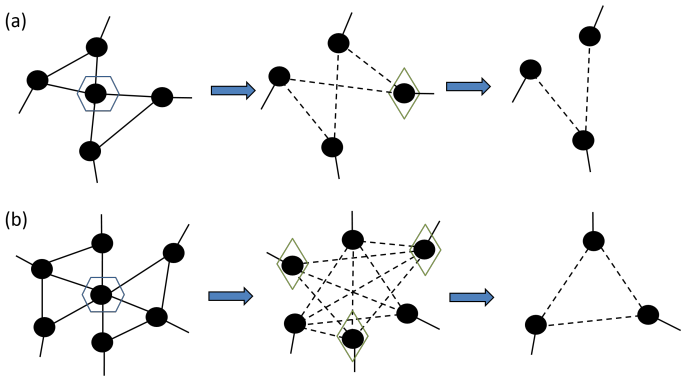

Figure 3 Illustration of graph transformation rules on Y measurements on a spin-2 domains and possible follow-up Z measurement to restore planarity. The hexagon indicates a Y-measured domain, and the diamonds indicate active Z measurements.

single site, but the quantum information remains the same (up to an inconsequential phase). But now if we continue to measure the second spin in the same way, this correponds to a logical X measurement and will change the entanglement structure for the remaining spins. In general, the effect of all $|\phi_\alpha^-\rangle\langle\phi_\alpha^-|$ (associated with K_α) in multi-site domains $\mathcal{C}$ is thus equivalent to a logical measurement of X operator.

Thus for each domain we need to distinguish two cases: (a) Fewer then all sites in an α-domain are affected by the POVM outcome K_α. Then, the domain is simply shrunk, and the graph G is unaffected. (b) All sites in an α-domain are affected by the POVM outcome K_α. Then, the encoded qubit residing on that domain is measured in the X-basis. If the latter happens, in terms of CGSB, measurement can be either a logical X or a logical Y measurement, and the state resulting from such measurement is again a graph state, and the new graph can be deduced from simple graph rules [7]; see Fig. 3 for illustration for Y-measurement.

4 Restoring planarity

We previously established simple criteria for computational universality of random planar graph states [16, 17], namely their corresponding graphs need to have a traversing path, and the domains need to be microscopic. The latter requirement for domains to be microscopic was checked numerically in several trivalent lattices [16, 17, 15] and also holds here via percolation argument. Therefore, what is needed to check is the former criterion. However, due to X- or Y-measured domains, the resultant graphs are no longer planer. After the POVM Eq. (1) we therefore apply a further round of active measurements with the purpose of restoring planarity of the encoded graph state.

What we choose to do here, specifically, is to first remove connected POVM "measured" (regardless of whether it is X- or Y-measured) domains by actively measuring their enclosing/neighboring domains in the logical Z basis, so as to remove these connected "measured" domains [7] at the cost of removing the enclosing domains as well. We also remove all X-measured domains and isolated *multi-site* (i.e. those with more than 2 sites) Y-measured domains by the same procedure. The non-planarity caused by these POVM "measured" domains is recovered quasi-locally; see Fig. 4.

Then we proceed to deal with the remaining isolated Y-measured domains which contain either one single or two sites (which can have at most 6 neighboring sites and hence domains).

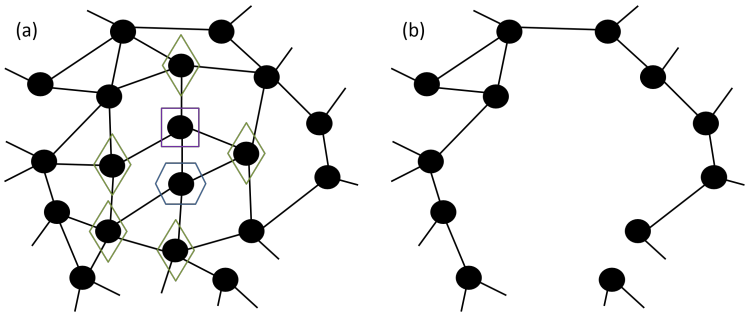

Figure 4 (color online) Part of a random graph for domains (solid circles). (a) The square indicates an X-measured domain and the hexagon indicates a Y-measured domain. In this example, the two measured domains are neighbors, and the effect on the graph will induce non-planarity. A simple approach is to apply active Z measurement on those domains (indicated by the diamonds) that enclose these connected X or Y-measured domains, similar to the game of go. (b) The upshot of the active Z measurements will remove these X/Y-measured domains as well as active Z-measured domains but will restore planarity.

The effect of Y-measured domains on the graph is to apply local complementation before removing the vertices corresponding to the Y-measured domains. If the Y-measured domain has three or fewer neighboring domains, the local complentation still preserves planarity. But when the nunber of neighbors is four or more, we then actively apply Z measurement on some of the neighboring domains (see Fig. 3) to maintain local planarity of the graph.

In the end we are left with a planar graph state, whose graph may or may not be percolated. If for large enough system and with finite nonzero probability, the graphs obtained after the above procedure are in the supercritical phase, then the resultant graph states can be used for universal MBQC, implying the original AKLT state is universal as well. Our simulations indicate that we need to use L of order 80 or larger in order to show that the graphs are in the supercritical phase with high probability such as 90%; see Fig. 5.

To carry out the simulations, we still need to sample the configuration $\{F, K\}$ according to the exact distribution $p(\{F, K\})$ [16]. In Section 5 we describe the formula.

5 Exact weight formula and simulation results

The exact sampling is needed, as random assignment of F and K POVM outcomes does not correctly reflect the correlation that these outcomes must obey due to multipartite entanglement in the AKLT state. Moreover, many of randomly chosen assignment of F and K are not valid measurement outcomes (as see below by the incompatibility condition). This latter complication sets the spin-2 case apart from the spin-3/2 case (in addition to the POVM itself). Employing the exact sampling also enables us to estimate the probability (at least the lower bound) of obtaining a universal resource state from performing the reduction procedure. We note that as long as the reduction procedure gives a finite, nonzero success probability in the large system limit then the original state is still regarded as a universal resource state (though of probabilistic nature). The weight formula that we discuss below will enable the exact sampling in the numerical simulations.

The weight formula. Let us recapitulate the notations introduced in Sec. 3.3. Consider a spin-2 AKLT state on a bi-colorable lattice $\mathcal{L}$ (generalization to non-bicolorable lattices is possible), and POVM elements F_α and K_α ($\alpha = x, y, z$). Denote by $J_F \subset \mathcal{L}$ the set of sites

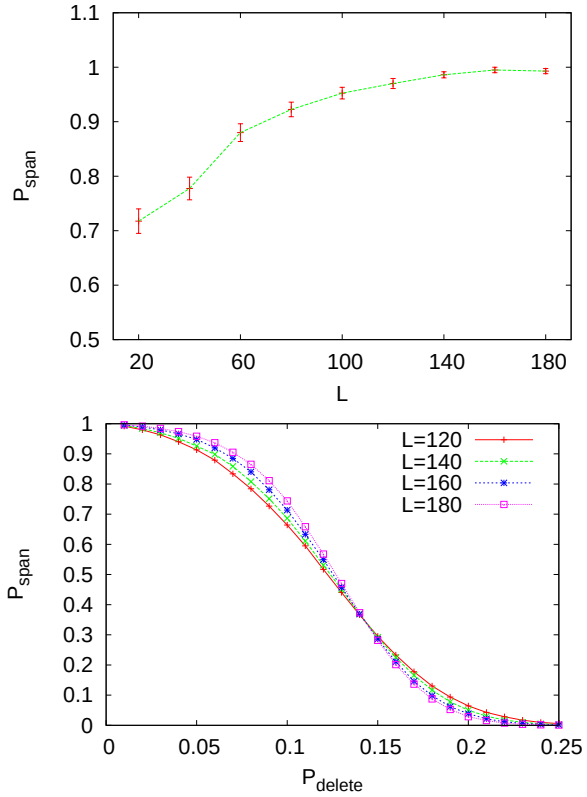

Figure 5 (a) Left panel: p_{span} vs. L (with $N = L^2$ the total number of sites) at $p_{\text{delete}} = 0$. As L increases p_{span} also increases. This is obtained with exact sampling. (b) Right panel: p_{span} vs. p_{delete} (with $N = L^2$ the total number of sites) with $L = 120, 140, 160, 180$. The threshold of p_{delete} is approximately 0.142(3). The crossing for these curves indicates that there is a percolation transition from the supercritical to subcritical phase in the thermodynamic limit.

where the POVM outcome is of F-type and by $J_K = \mathcal{L}\backslash J_F$ the set of sites where POVM outcome is of K-type. Here additionally we denote by D_K the set of *domains* where the number of K-type POVM elements is equal to the total number of sites in the domain. Denote $\{F, K\}$ the set of POVM outcomes corresponding to $F^{(v)}_{\alpha(v)}$ and $K^{(w)}_{\beta(w)}$ and the probability for such occurrence is $p(\{F, K\})$.

We have introduced the graph state $|G_0\rangle$ in Eq. (4). Let us also label the set of all domains (i.e. vertices of the G_0) by V, the set of all inter-domain edges in $\mathcal{L}$ by $\mathcal{E}$ and the set of all edges of G_0 by E. Note that E is obtained from $\mathcal{E}$ by a modulo-2 operation [16].

As explained in Sec. 3.3, the effect of K-type POVM elements on a strict subset of sites in a domain only shrinks the size of a domain, whereas K-type POVM measurement on *all* sites in a domain in D_K amounts to the measurement (on $|G_0\rangle$) of an encoded logical X with respect to the encoding in Table 2. The stablizer operators for $|G_0\rangle$ in this encoding can be either $\pm X_c \bigotimes_{\mu\in \text{Nb}(c)} Z_\mu$ or $\pm Y_c \bigotimes_{\mu\in \text{Nb}(c)} Z_\mu$ (see Appendix 3.2), where $\text{Nb}(c)$ denotes the set of neighbors of vertex c. But one can perform local logical-qubit rotations such that all stabilizer operators are of the canonical form $X_c \bigotimes_{\mu\in \text{Nb}(c)} Z_\mu$, but then the effect of K-type POVM elements in a domain inside D_K amounts to the measurement of an encoded observable either X or Y. We have referred to this latter basis as the canonical graph-state basis (CGSB) earlier.

Now we introduce a $|V| \times |D_K|$ binary-valued matrix H with its entries defined as follows,

$$H_{\mu\nu} = 0, \text{ if } [\mathcal{K}_\mu, O_\nu] = 0, \tag{10a}$$
$$H_{\mu\nu} = 1, \text{ if } \{\mathcal{K}_\mu, O_\nu\} = 0, \tag{10b}$$

where $\mathcal{K}_\mu$ is the stabilizer operator associated with the vertex (or domain) $\mu \in V$ of the graph G, $O_\nu \equiv (-1)^{|V_\mu|} X_\mu$ is proportional to a logical Pauli X operator, and $\nu \in D_K$; see also Sec. 3.2. Let $\dim\big(\ker(H)\big)$ denote the dimension of the kernel of matrix H. We are ready to introduce the following lemma.

▶ **Lemma 1.** *If there exists a set Q (subset of D_K) such that $-\otimes_{\mu\in Q} O_\mu$ is in the stablizer group $\mathcal{S}(|G_0\rangle)$ of the state $|G_0\rangle$, then $p(\{F,K\}) = 0$. Otherwise,*

$$p(\{F,K\}) = c \left(\frac{1}{2}\right)^{|\mathcal{E}|-|V|+2|J_K|-\dim\left(\ker(H)\right)}, \tag{11}$$

where c is a constant.

We subsequently refer to the above condition for $p(\{F,K\}) = 0$ as the *incompatability condition*. The incompatibility condition implies that not all POVM outcomes labeled by F_α and K_α can occur. When there is no K outcome, Eq. (11) reduces to $p = c\, 2^{|V|-|\mathcal{E}|}$ of previous results [16]. The correlation of F's and K's at different sites is reflected either in the incompatibility condition (if it is met) or else in the factor $\dim\big(\ker(H)\big)$. The probability distribution of $\{F,K\}$ is thus very far from independent and random. For the proof of the lemma, see Appendix A.

Numerical simulations. With the weight formula we can sample the exact distribution of physically allowed POVM outcomes $\{F,K\}$ and carry out the procedure to restore planarity of the random graphs associated with the post-POVM states. The sampling is obtained by using the standard Metropolis algorithm for updating $\{F,K\}$ configurations. One notable distinction is that we will need to avoid configurations that satisfies the incompatibility condition. First, we check whether the random graphs after our procedure have a spanner cluster by showing p_{span} for different L, and we see that it increases as L increases and approaches to unity; see Fig. 5. This suggests that for L large enough, the random graphs resulting from the thinning procedure are percolated. Then, we perform site percolation numerical experiment on these random graphs by removing each vertex with a probability p_{delete} and record the probability of a spanning cluster p_{span}. The crossing of curves in Fig. 5 for different sizes indicates that there is a percolation transition (at $p^*_{\text{delete}} \approx 0.142$) from the supercritical to subcritical phase in the thermodynamic limit. This shows that our random graph states (whose graphs are sitting at $p_{\text{delete}} = 0$) can be used to generate a network of entanglement that is universal for measurement-based quantum computation. This shows that the original AKLT state is also universal.

6 Concluding remarks

The family of Affleck-Kennedy-Lieb-Tasaki states provides a versatile playground for universal quantum computation. The merit of these states is that by appropriately choosing boundary conditions they are unique ground states of two-body interacting Hamiltonians, possibly with a spectral gap above the ground states. Here we have overcome several obstacles and

shown that the spin-2 AKLT state on the square lattice is also a universal resource for measurement-based quantum computation. We were able to derive an exact weight formula for any given POVM outcome. Combined with a thinning procedure to restore planarity of random graph states, we performed Monte Carlo simulations and demonstrated that the assoicated planar random graphs from the procedure are residing in the supercritical phase.

The emerging picture from our series of study on the quantum computational universality in the two-dimensional AKLT valence-bond family is as follows. AKLT states involving spin-2 and other lower spin entities are universal if they reside on a two-dimensional frustration-free regular lattice with any combination of spin-2, spin-3/2, spin-1 and spin-1/2 (consistent with the lattice). Additionally, the effect of frustrated lattice may not be serious and can always be decorated (by adding additional spins) such that the resultant AKLT state is universal. We conjecture that the result hold in three dimensions as well.

Another direction of generalization is to investigate the robustness of the resource under small perturbations, e.g., slightly away from the AKLT Hamiltonian. A slight and simpler variation [5] is to consider the AKLT deformed spin-2 AKLT state with some deformation parameters, for which we give more detail in our arXiv paper [20]. One can also consider the frustrated kagomé lattice and deform it in a way to connect to a cluster state [4]. Furthermore, how would the quantum computational power of AKLT-like states make transition and how would they compare with the usual phases of matter [19]. We leave these for future consideration.

Acknowledgements. This work was supported by the National Science Foundation under Grants No. PHY 1314748 and No. PHY 1333903 (T.-C. W.) and by NSERC, Cifar and IARPA (R. R.).

References

1 H. J. Briegel, D. E. Browne, W. Dür, R. Raussendorf, and M. Van den Nest, Nature Phys. **5**, 19 (2009).
2 J.-M. Cai, A. Miyake, W. Dür, and H. J. Briegel, Phys. Rev. A **82**, 052309 (2010).
3 X. Chen, B. Zeng, Z.-C. Gu, B. Yoshida, and I. L. Chuang, Phys. Rev. Lett. **102**, 220501 (2009).
4 A. S. Darmawan and S. D. Bartlett , New J. Phys. **16**, 073013 (2014).
5 A. S. Darmawan, G. K. Brennen, and S. D. Bartlett, New J. Physics, **14**, 013023 (2012).
6 D. Gross and J. Eisert, Phys. Rev. Lett. **98**, 220503 (2007).
7 M. Hein, W. Dur, J. Eisert, R. Raussendorf, M.Van den Nest, and H.-J. Briegel, in *Quantum Computers, Algorithms and Chaos*, edited by G. Casati, D. Shepelyansky, P. Zoller, and G. Benenti, International School of Physics Enrico Fermi Vol. 162 (IOS Press, Amsterdam, 2006); also in arXiv:quant-ph/0602096.
8 R. Kaltenbaek, J. Lavoie, B. Zeng, S. D. Bartlett, and K. J. Resch, Nature Physics **6**, 850 (2010).
9 Ç. K. Koç and S. N. Arachchige, J. Parallel and Distributed Computing **13**, 118 (1991).
10 See e.g. the review by L. C. Kwek, Z. Wei, and B. Zeng, Int. J. Mod. Phys. B **26**, 1230002 (2012).
11 A. Miyake, Ann. Phys. (Leipzig) **326**, 1656 (2011).
12 M. A. Nielsen, Rep. Math. Phys. **57**, 147 (2006).
13 R. Raussendorf and H. J. Briegel, Phys. Rev. Lett. **86**, 5188 (2001).
14 R. Raussendorf and T.-C. Wei, Annual Review of Condensed Matter Physics **3**, pp.239-261 (2012).
15 T.-C. Wei, Phys. Rev. A **88**, 062307 (2013).

16 T.-C. Wei, I. Affleck, and R. Raussendorf, Phys. Rev. Lett. **106**, 070501 (2011).
17 T.-C. Wei, I. Affleck, and R. Raussendorf, Phys. Rev. A **86**, 032328 (2012).
18 T.-C. Wei, P. Haghnegahdar, R. Raussendorf, Phys. Rev. A **90**, 042333, (2014).
19 T.-C. Wei, Y. Li, and L. C. Kwek, Phys. Rev. A **89**, 052315 (2014).
20 T.-C. Wei and R. Raussendorf, arXiv:1501.07571.

A Proof of the weight formula

Let us mention first the following fact that (b is chosen according to a_c in Table 1),

$$\langle G_0|O_{\rm rest}\otimes_{i\in I_c}\sigma_b^{[i]}|G_0\rangle=0, \tag{12}$$

if I_c is a strict subset of virtual qubits in any domain $\mathcal{C}$ (i.e. $|I_c|<4|\mathcal{C}|$) and σ_b is chosen according to Table 1 ($O_{\rm rest}$ denotes operators not in the support of domain $\mathcal{C}$). This can easily be proved by the fact that one can choose a stabilizer $S_{jq}\equiv\lambda_j\lambda_q\sigma_{a_c}^{[j]}\sigma_{a_c}^{[q]}$ (see Table 2), where $j\in I_c$ and $q\in\mathcal{C}$ but $q\notin I_c$, so that $(\otimes_{i\in I_c}(\sigma_b^{[i]})$ and S_{jq} anticommutes. Hence,

$$\begin{aligned}&\langle G_0|O_{\rm rest}(\otimes_{i\in I_c}\sigma_b^{[i]})|G_0\rangle=\langle G_0|O_{\rm rest}(\otimes_{i\in I_c}\sigma_b^{[i]})S_{jk}|G_0\rangle\\ =\;&-\langle G_0|S_{jk}O_{\rm rest}(\otimes_{i\in I_c}\sigma_b^{[i]})|G_0\rangle=-\langle G_0|O_{\rm rest}(\otimes_{i\in I_c}\sigma_b^{[i]})|G_0\rangle,\end{aligned}$$

showing that the expectation value is identically zero.

Let us also note the following useful relation regarding to the 4-qubit GHZ associated with the corresponding POVM outcome K_α,

$$|{\rm GHZ}_\alpha^-\rangle\langle{\rm GHZ}_\alpha^-|=\Pi_\alpha\frac{(1-\sigma_{b_\alpha}^{[v;1]}\sigma_{b_\alpha}^{[v;2]}\sigma_{b_\alpha}^{[v;3]}\sigma_{b_\alpha}^{[v;4]})}{2}\Pi_\alpha, \tag{13}$$

where Π_α ($\alpha=x,y,z$) is a projection to a two-dimensional subspace, equivalently an identity operator on the code subspace and can be safely omitted when acting on the graph state $|G_0\rangle$. Specificially, $\Pi_x=|++++\rangle\langle++++|+|----\rangle\langle----|$, $\Pi_y=|i,i,i,i\rangle\langle i,i,i,i|+|-i,-i,-i,-i\rangle\langle -i,-i,-i,-i|$ and $\Pi_z=|0000\rangle\langle 0000|+|1111\rangle\langle 1111|$. The label b_α denotes the corresponding type b if $a_c=\alpha$; see Table 1.

For a given domain (with a given type α), the POVM outcome on any site in the domain can be either F_α or K_α. Regarding the number n_K of K outcomes, there are two scenarios: (i) n_K is less than the total number $|V_c|$ of sites in that domain $\mathcal{C}$; (ii) $n_K=|V_c|$.

For case (i), the effect of all those K in terms of the probability distribution (or the weight formula) is to multiply a factor of 2^{-n_K}, i.e., (using $J\in\mathcal{C}$ to denotes the set of those sites with K)

$$\begin{aligned}&\langle G_0|O_{\rm rest}\left(\otimes_{v\in J}|{\rm GHZ}_{\alpha(v)}^-\rangle\langle{\rm GHZ}_{\alpha(v)}^-|\right)|G_0\rangle=\langle G_0|O_{\rm rest}\otimes_{v\in J}\frac{(1-\sigma_b^{[v;1]}\sigma_b^{[v;2]}\sigma_b^{[v;3]}\sigma_b^{[v;4]})}{2}|G_0\rangle\\ =&2^{-n_K}\langle G_0|O_{\rm rest}|G_0\rangle,\end{aligned}$$

where $O_{\rm rest}$ denotes operators not in the support of domain $\mathcal{C}$, and we have used

$$\langle G_0|O_{\rm rest}\otimes_{v\in J}(\sigma_b^{[v;1]}\sigma_b^{[v;2]}\sigma_b^{[v;3]}\sigma_b^{[v;4]})|G_0\rangle=0.$$

For case (ii), when we expand all the $2^{|V_c|}$ terms in $\otimes_{v\in\mathcal{C}}(1-\sigma_b^{[v;1]}\sigma_b^{[v;2]}\sigma_b^{[v;3]}\sigma_b^{[v;4]})/2$, the only two nonvanishing contributions are $1/2^{|V_c|}$ and $(-1)^{|V_c|}(\otimes_{i=1}^{4|\mathcal{C}|}\sigma_b^{[i]})/2^{|V_c|}=(-1)^{|V_c|}X_c/2^{|V_c|}$.

In terms of logical X, the effect of all K is equivalent to $P_c = (1 + O_c)/2^{|V_c|}$, where the $O_c = (-1)^{|V_c|} X_c$. That is

$$\langle G_0|O_{\rm rest}\left(\otimes_{v\in C}|{\rm GHZ}^-_{\alpha(v)}\rangle\langle{\rm GHZ}^-_{\alpha(v)}|\right)|G_0\rangle = \langle G_0|O_{\rm rest}\otimes_{v\in C}\frac{(1-\sigma_b^{[v;1]}\sigma_b^{[v;2]}\sigma_b^{[v;3]}\sigma_b^{[v;4]})}{2}|G_0\rangle$$
$$= 2^{-|V_c|}\langle G_0|O_{\rm rest}(1+O_c)|G_0\rangle.$$

Here we also see that the effect of all K in domain $\mathcal{C}$ is to measurement the logical qubit $\mathcal{C}$ in the logical X, followed by a post-selection of the result corresponding to either positive (if $|V_c|$ is even) or negative (if $|V_c|$ is oddd) eigenvalue of X.

With the above preparation, we can move on to the proof. Now consider a spin-2 AKLT state on a bi-colorable lattice $\mathcal{L}$ (generalization to non-bicolorable lattices is possible), and POVM elements F_α and K_α ($\alpha = x, y, z$). Denote by $J_F \subset \mathcal{L}$ the set of sites where the POVM outcome is of F-type and by $J_K = \mathcal{L}\backslash J_F$ the set of sites where POVM outcome is of K-type. We should, strictly speaking, use $\alpha(v)$ to denote the type of x, y, z at site v. When there is no confusion, we simply write α.

Proof of Lemma 1. For simplicity let us denote the AKLT state by $|\psi\rangle$ below. The probability $p(\{F, K\})$ for obtaining POVM measurements $\{F, K\}$ described above is

$$p(\{F,K\}) = \langle\psi|\bigotimes_{v\in J_F} F^{(v)\dagger}_{\alpha(v)}F^{(v)}_{\alpha(v)}\bigotimes_{w\in J_K}K^{(w)\dagger}_{\alpha(w)}K^{(w)}_{\alpha(w)}|\psi\rangle$$
$$= \left(\frac{3}{2}\right)^{|J_K|}\langle\psi|\bigotimes_{v\in J_F} F^{(v)\dagger}_{\alpha(v)}F^{(v)}_{\alpha(v)}\bigotimes_{w\in J_K}F^{(w)\dagger}_{\alpha(w)}K^{(w)\dagger}_{\alpha(w)}K^{(w)}_{\alpha(w)}F^{(w)}_{\alpha(w)}|\psi\rangle$$
$$= \left(\frac{1}{2}\right)^{|J_K|}\langle\psi|\bigotimes_{v\in\mathcal{L}} F^{(v)\dagger}_{\alpha(v)}\bigotimes_{w\in J_K}|{\rm GHZ}^-_{\alpha(w)}\rangle\langle{\rm GHZ}^-_{\alpha(w)}|\bigotimes_{u\in\mathcal{L}}F^{(u)}_{\alpha(u)}|\psi\rangle.$$

In the second equality we have used the fact that $K_\alpha = \sqrt{3/2}K_\alpha F_\alpha$, and in the third equality we have combined all F's and written explicitly K_α's in terms of the four-qubit GHZ projectors.

Now we know from Ref. [16] that

$$\bigotimes_{u\in\mathcal{L}}F^{(u)}_{\alpha(u)}|\psi\rangle = c_0\left(\frac{1}{\sqrt{2}}\right)^{|\mathcal{E}|-|V|}|G_0\rangle, \tag{14}$$

where $|G_0\rangle$ is an encoded graph state whose graph G_0 is specified by the POVM elements $\{F\}$, V is the set of domains of same-outcome POVM measurements, and $\mathcal{E}$ is the set of inter-domain edges (before the modulo-2 operation) [16]. The formula (14) was originally stated for the honeycomb lattice, but holds for all bipartite lattices. (For non-bipartite lattices, an additional condition needs to be imposed relating to geometric frustration [15]. Namely, if any domain contains a cycle with odd number of sites, such $\{F\}$ will not appear.) Combining the above two results we find that

$$p(\{F,K\}) = |c_0|^2\left(\frac{1}{2}\right)^{|\mathcal{E}|-|V|+|J_K|}\times\langle G_0|\left(\bigotimes_{v\in J_K}|{\rm GHZ}^-_{\alpha(v)}\rangle\langle{\rm GHZ}^-_{\alpha(v)}|\right)|G_0\rangle. \tag{15}$$

Using Eq. (13) and the results in the beginning of the section, we know that for those GHZ-projections in a domain such that their number is less than the total number of sites in the domain, i.e., case (i) discussed above, their contribution is to mulitiply by a factor 2^{-n_K}. For those such that the two numbers are equal, i.e., case (ii), these GHZ-projections (in a

domain) can be replaced by $P_c = (1 + O_c)/2^{|V_c|}$, where the $O_c = (-1)^{|V_c|} X_c$, and c labels the domain. Thus,

$$p(\{F, K\}) = |c_0|^2 \left(\frac{1}{2}\right)^{|\mathcal{E}|-|V|+2|J_K|} \times \langle G_0| \bigotimes_{c\in D_K} (I_c + O_c)|G_0\rangle, \tag{16}$$

where we use D_K to label the domains that contain the same number of K operators as the total number of internal sites.

Next we demonstrate the first part of the Lemma. Assume that, for some subset $Q \in D_K$, the observable $-\otimes_{c\in Q} O_c \in \mathcal{S}(|G_0\rangle)$. Then,

$$\begin{aligned} & \langle G_0| \bigotimes_{\mu\in D_K} (I_\mu + O_\mu)|G_0\rangle = \langle G_0| \bigotimes_{\nu\in D_K\setminus Q} (I_\nu + O_\nu) \bigotimes_{\mu\in Q} (I_\mu + O_\mu) \left(- \bigotimes_{c\in Q} O_c\right) |G_0\rangle \\ = \quad & -\langle G_0| \bigotimes_{\nu\in D_K\setminus Q} (I_\nu + O_\nu) \bigotimes_{c\in Q} (O_c + I_c)|G_0\rangle = -\langle G_0| \bigotimes_{\mu\in D_K} (I_\mu + O_\mu)|G_0\rangle = 0. \end{aligned}$$

In the third line we have used the fact $O_\mu^2 = I_\mu$. Let us also note that being product of Pauli operators, O_μ either commutes or anticommutes with another product of Pauli operators.

Next, we demonstrate the second part of the Lemma, i.e., finding $p(\{F, K\})$ when it is not identically zero. Consider a subset of domains $Q \subset D_K$. If $\otimes_{\mu\in Q} O_\mu \notin \pm\mathcal{S}(|G_0\rangle)$, then $\langle G_0| \otimes_{\mu\in Q} O_\mu |G_0\rangle = 0$ (note that μ is an index for the domain, not an index for the site). Furthermore, if the incompatibility condition is not satisfied, then $\otimes_{\mu\in Q} O_\mu \in \pm\mathcal{S}(|G_0\rangle)$ implies that $\otimes_{\mu\in Q} O_\mu \in \mathcal{S}(|G_0\rangle)$, and therefore $\langle G_0| \otimes_{\mu\in Q} O_\mu |G_0\rangle = 1$. We now exapnd the projector $\otimes_{c\in D_K}(I_c + O_c)$ in the matrix element,

$$\langle G_0| \bigotimes_{c\in D_K} (I_c + O_c)|G_0 = \langle G_0| \sum_{Q\subset D_K} \bigotimes_{\mu\in Q} O_\mu |G_0\rangle = |M|, \tag{17}$$

where the set M is defined as $M = \{O(Q) \equiv \otimes_{\mu\in Q} O_w | Q \subset D_K \,\text{and}\, O(Q) \in \mathcal{S}(|G_0\rangle)\}$. Actually M has the following equivalent formulation which will turn out to be useful,

$$M = \{O(Q) \equiv \bigotimes_{\mu\in Q} O_\mu | Q \subset D_K \;\text{ and}\, [O(Q), S] = 0, \forall S \in \mathcal{S}(|G_0\rangle)\}. \tag{18}$$

Using this latter characterization of M, we now turn to the counting for $|M|$. We describe every subset Q of D_K by its characteristic vector $\mathbf{q}$, defined as follows: if $\mu \in Q$ then $q_\mu = 1$, or if $\mu \notin Q$, then $q_\mu = 0$. Furthermore we define a binary-valued matrix H of dimension $|V| \times |D_K|$ (where $|V|$ denotes total number of domains), whose entries are

$$\begin{aligned} & H_{\mu\nu} = 0, \text{ if } [\mathcal{K}_\mu, O_\nu] = 0, \\ & H_{\mu\nu} = 1, \text{ if } \{\mathcal{K}_\mu, O_\nu\} = 0, \end{aligned}$$

where $\mu \in V$ (the set of all domains) and $\nu \in D_K$ (the set of those domains with equal number of K's and sites). Then for any $Q \subset D_K$, $O(Q) \in M$ if and only if $H\mathbf{q} \bmod 2 = \mathbf{0}$. Therefore,

$$|M| = 2^{\dim\left(\ker(H)\right)}. \tag{19}$$

Putting everything into the expression for $p(\{F, K\})$ we obtain the equation (11),

$$p(\{F, K\}) = |c_0|^2 \left(\frac{1}{2}\right)^{|\mathcal{E}|-|V|+2|J_K|-\dim\left(\ker(H)\right)},$$

and the lemma is proved. ◀

We remark that checking the kernel of a binary matrix can be done via, e.g., the Gauss elimination method; see e.g. [9]. Furthermore, to check the incompatibility condition it is sufficient to check the products of O_μ associated with all basis vectors $\mathbf{q}$'s in the kernel. If none of them satisifies it, then the incompatibility condition is not satisified.